

# Indirect and Direct Detection of the 4-(Benzothiazol-2-yl)phenylnitrenium Ion from a Putative Metabolite of a Model Anti-Tumor Drug

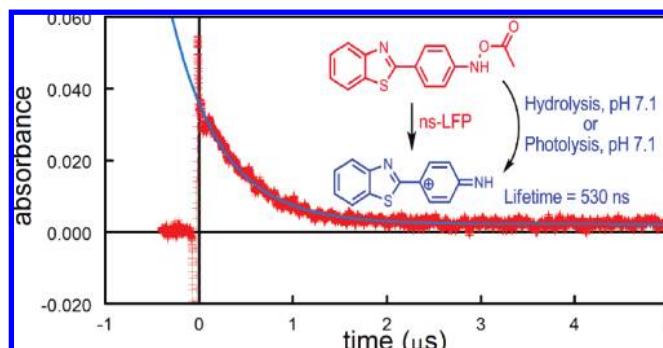
Mrinal Chakraborty,<sup>†</sup> Kyoung Joo Jin,<sup>†</sup> Samuel C. Brewer III,<sup>†</sup> Huo-Lei Peng,<sup>‡</sup> Matthew S. Platz,<sup>‡</sup> and Michael Novak<sup>\*,†</sup>

Department of Chemistry and Biochemistry, Miami University, Oxford, Ohio 45056,  
and Department of Chemistry, The Ohio State University, 100 West 18th Avenue,  
Columbus, Ohio 43210

novakm@muohio.edu

Received August 24, 2009

## ABSTRACT



2-(4-Aminophenyl)benzothiazoles related to **1** are potentially important pharmaceuticals. Metabolism apparently involves oxidation and esterification to **3**. In water, hydrolysis and photolysis of **3** generates the nitrenium ion **4** that can be detected indirectly by  $N_3^-$  trapping and directly by UV–vis spectroscopy following laser flash photolysis. The transient, with  $\lambda_{\max}$  570 nm, and a lifetime of 530 ns, reacts with  $N_3^-$  at a diffusion-controlled rate and generates the quinol **6** by reaction with water.

Benzothiazole derivatives such as 2-(4-aminophenyl)benzothiazole, **1**, are under investigation as antitumor, antifungal, and antibacterial agents,<sup>1–3</sup> and as radiopharmaceuticals for binding and in vivo imaging of A $\beta$ -plaques, one of the earliest pathological processes in the development of Alzheimer's

disease.<sup>4</sup> One antitumor derivative of **1** is currently in phase 1 clinical trials in Great Britain.<sup>5</sup> The use of **1** and its derivatives as antitumor agents requires biological activation.<sup>5,6</sup> The proposed metabolism of **1** to form the active agent **3** is shown in Scheme 1, although neither **2** nor **3** had been isolated and characterized. It is presumed that **3** further

<sup>†</sup> Miami University.

<sup>‡</sup> The Ohio State University.

(1) Shi, D.-F.; Bradshaw, T. D.; Wrigley, S.; McCall, C. J.; Lelieveld, P.; Fichtner, I.; Stevens, M. F. G. *J. Med. Chem.* **1996**, *39*, 3375–3384. Bradshaw, T. D.; Wrigley, S.; Shi, D.-F.; Schultz, R. J.; Paull, K. D.; Stevens, M. F. G. *Br. J. Cancer* **1998**, *77*, 745–752. Hutchinson, I.; Jennings, S. A.; Vishnuvajjala, B. R.; Westwell, A. D.; Stevens, M. F. G. *J. Med. Chem.* **2002**, *45*, 744–747.

(2) Yildiz-Oren, I.; Yalcin, I.; Aki-Sener, E.; Ucarturk, N. *Eur. J. Med. Chem.* **2004**, *39*, 291–298.

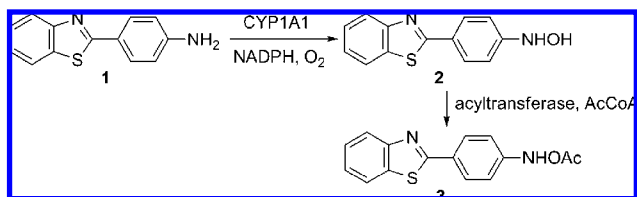
(3) Ra, C. S.; Jung, B. Y.; Park, G. *Heterocycles* **2004**, *62*, 793–802.

(4) Tzanopoulou, S.; Pirmettis, I. C.; Patsis, G.; Paravatou-Petsotas, M.; Livaniou, E.; Papadopoulos, M.; Pelecanou, M. *J. Med. Chem.* **2006**, *49*, 5408–5410.

(5) Bradshaw, T. D.; Westwell, A. D. *Curr. Med. Chem.* **2004**, *11*, 1009–1021. Brantley, E.; Antony, S.; Kohlhaagen, G.; Meng, L.; Agama, K.; Stinson, S. F.; Sausville, E. A.; Pommier, Y. *Cancer Chemother. Pharmacol.* **2006**, *58*, 62–72.

(6) Chua, M.-S.; Kashiwayama, E.; Bradshaw, T. D.; Stinson, S. F.; Brantley, E.; Sausville, E. A.; Stevens, M. F. G. *Cancer Res.* **2000**, *60*, 5196–5203.

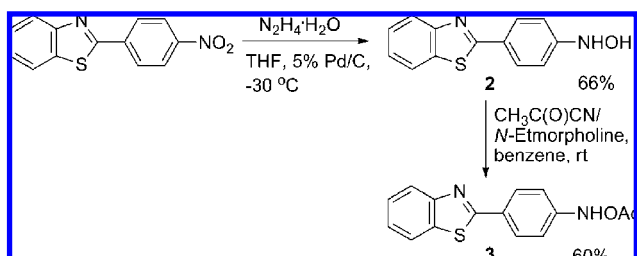
**Scheme 1.** Proposed Metabolism of **1**



decomposes into a reactive electrophile, but no direct evidence for this proposal has been presented.<sup>7</sup>

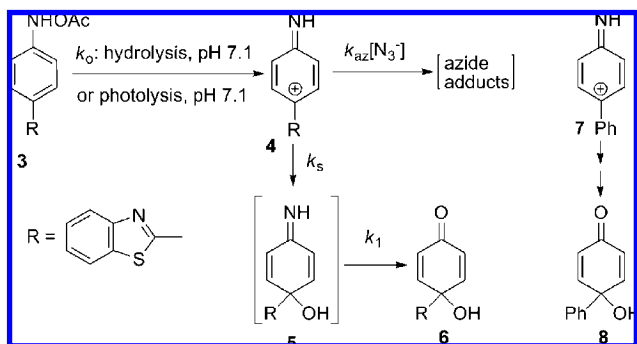
We have succeeded in synthesizing both **2** and **3** from 2-(4-nitrophenyl)benzothiazole using procedures we previously developed for making similar derivatives of carcinogenic aromatic amines (Scheme 2).<sup>8</sup> Reduction of the nitro

**Scheme 2.** Synthesis of **2** and **3**



compound<sup>9</sup> with hydrazine hydrate in the presence of 5% Pd/C catalyst generates **2** in moderate yield, while treatment of **2** with acetyl cyanide in the presence of *N*-ethylmorpholine provides **3** in satisfactory yield. We now report the indirect and direct detection of nitrenium ion **4** (Scheme 3) from hydrolysis and photolysis of **3**.

**Scheme 3.** Kinetic Scheme for **3** and **4**



Kinetics of the decomposition of **3** ( $2.5 \times 10^{-5}$  M) at pH 7.1 in phosphate buffer, and the formation of the major hydrolysis product **6** (Scheme 3, identified by HPLC and <sup>1</sup>H NMR comparison to an authentic sample<sup>10</sup>) monitored

by UV spectroscopy, are described by two pseudo-first-order rate constants,  $k_0$  and  $k_1$ . HPLC studies (Figure 1A) show

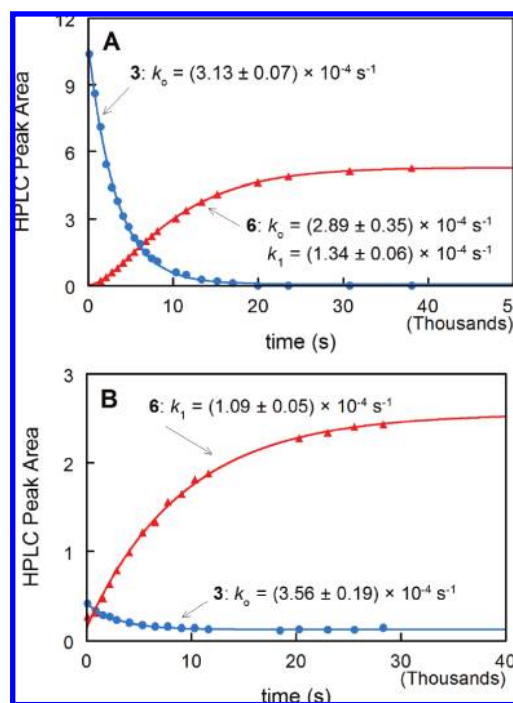


**Figure 1.** Time course for the disappearance of **3** and formation of **6** at 10 °C in pH 7.1 phosphate buffer monitored by HPLC with UV detection at 212 nm: (A) hydrolysis reaction in the dark and (B) after steady-state photolysis for 30 s. Rate constants were obtained from fits to single or double exponential rate equations.

that the larger rate constant,  $k_0$  governs the decay of **3**, while the appearance of **6** is biphasic, and is fit well by a rate equation for two consecutive first-order reactions. The larger rate constant generated by the fit is equivalent in magnitude to  $k_0$  measured for the disappearance of **3**. The rate of appearance of **6** is limited by the smaller rate constant,  $k_1$ . Kinetics of the appearance of **6** are consistent with its formation from a long-lived intermediate (lifetime ca. 2 h at 10 °C) that is generated by hydrolysis of **3**. Steady-state photolysis of an identical aqueous solution of **3** for 30 s with UVB lamps leads to photodecomposition of 96% of **3** (Figure 1B). Generation of **6** now occurs via a simple first-order process governed by  $k_1$ . Correction for the small amount of **3** remaining after photolysis shows that 92% of the observed yield of **6** under photolysis conditions is due to photodecomposition of **3**.

(7) O'Brien, S. E.; Browne, H. L.; Bradshaw, T. D.; Westwell, A. D.; Stevens, M. F. G.; Laughton, C. A. *Org. Biomol. Chem.* **2003**, *1*, 493–497. Hilal, R.; Khalek, A. A. A.; Elrobby, S. A. K. *THEOCHEM* **2005**, *731*, 115–121.

(8) Kazerani, S.; Novak, M. *J. Org. Chem.* **1998**, *63*, 895–897. Novak, M.; Kazerani, S. *J. Am. Chem. Soc.* **2000**, *122*, 3606–3616.

(9) Stevens, M. F. G.; Shi, D.-F.; Castro, A. *J. Chem. Soc., Perkin Trans. I* **1996**, 83–93.

(10) Wang, Y.-T.; Jin, K. J.; Myers, L. R.; Glover, S. A.; Novak, M. *J. Org. Chem.* **2009**, *74*, 4463–4471.

The results show that **6** is generated both by hydrolysis and photolysis of **3**, and suggest that a common pathway is involved in both processes.

Addition of  $\text{N}_3^-$  to the hydrolysis solution does not affect the rate of decomposition of **3**, but does significantly decrease the yield of **6** at very low  $[\text{N}_3^-]$  (Figure 2), demonstrating

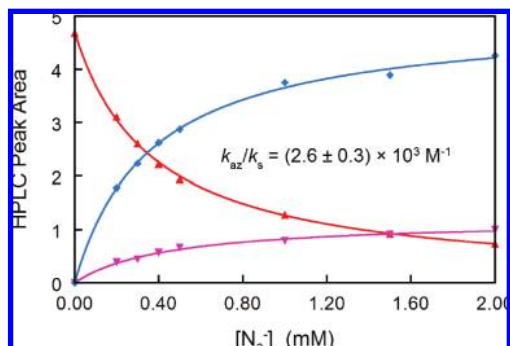


**Figure 2.** Results of azide trapping experiment in pH 7.1 phosphate buffer at 30 °C. Key: **6** ( $\blacktriangle$ , 212 nm), apparent major azide adduct ( $\blacklozenge$ , 330 nm), and apparent minor azide adduct ( $\blacktriangledown$ , 212 nm). The  $k_{\text{az}}/k_s$  is the average of the fit of all three materials to the standard “azide clock” formulas.

that  $\text{N}_3^-$  traps a reactive intermediate produced in a rate limiting step. As the yield of **6** decreases, the yields of two new products, not generated in the absence of  $\text{N}_3^-$ , increase. Application of the “azide clock” equations<sup>11</sup> to the yields of these three products generates the experimental  $k_{\text{az}}/k_s$  shown in Figure 2. Although the azide products have not yet been characterized, the structure of **6** and the trapping results show that  $\text{N}_3^-$  competes with the solvent for a selective cationic intermediate, **4**. The kinetics of the formation of **6** during hydrolysis of **3** implicates **5** as a precursor, although **5** has not yet been detected.

Laser flash photolysis (LFP) of **3** in  $\text{O}_2$ -saturated pH 7.1 phosphate buffer at 308 nm generates a transient UV spectrum with  $\lambda_{\text{max}}$  ca. 570 nm (Figure 3). The absorbance

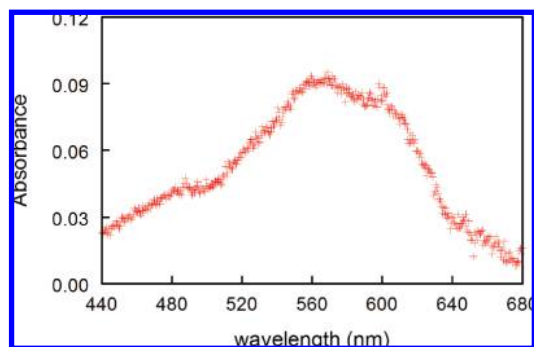


**Figure 3.** Transient absorbance spectrum obtained 20 ns after 308 nm excitation of **3** in  $\text{O}_2$ -saturated pH 7.1 phosphate buffer. The spectrum was recorded with a 20 ns window.

at 570 nm decays in a first-order manner (Supporting Information, Figure S1). The rate constant,  $k_{\text{obs}}$ , increases linearly with increasing  $[\text{N}_3^-]$  (Figure 4).

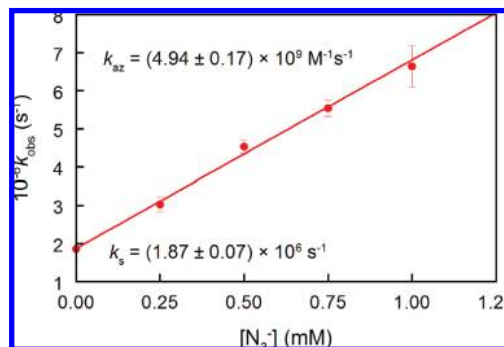


**Figure 4.** Plot of  $k_{\text{obs}}$  from LFP experiments vs.  $[\text{N}_3^-]$ . Data were fit by a weighted least-squares procedure to obtain  $k_s$  and  $k_{\text{az}}$ . The adjusted  $r^2 = 0.9967$ .

The slope of that plot is  $k_{\text{az}}$ , the second-order rate constant for reaction of  $\text{N}_3^-$  with the reactive intermediate, while the intercept is  $k_s$ , the pseudo-first-order rate constant for reaction of the intermediate with the aqueous solvent. The ratio  $k_{\text{az}}/k_s$  of  $(2.64 \pm 0.13) \times 10^3 \text{ M}^{-1}$  is identical with that obtained from the azide-trapping experiments, demonstrating that both experiments detect the same intermediate, **4**, with a lifetime ( $1/k_s$ ) of ca. 530 ns.

Scheme 3 summarizes the results of our experiments. This scheme is similar to that previously demonstrated for the decomposition of ester derivatives of carcinogenic aromatic hydroxylamines.<sup>12</sup> The cation **4** is about as selective as the 4-biphenylnitrenium ion, **7** ( $k_{\text{az}}/k_s = 2.9 \times 10^3 \text{ M}^{-1}$ ), that also yields a quinol, **8**, as its major hydration product.<sup>12</sup> The intermediate detected after LFP is definitely **4**, not the imine **5**, because the kinetics performed by UV spectroscopy and HPLC show that **5** has a lifetime of about 30 min at room temperature, while the transient generated during the LFP experiments has a lifetime of 530 ns.

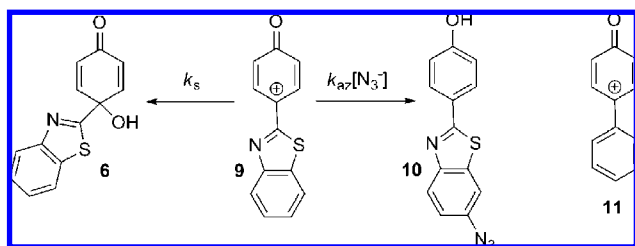
An apparent imine intermediate can be detected by HPLC during the conversion of **7** into **8**.<sup>12</sup> This species has a lifetime of ca. 6 h at room temperature, while **7** has a lifetime of 560 ns under the same conditions.<sup>12</sup> The quinol product **6** is also the hydration product of the related oxenium ion **9** (Scheme 4).<sup>10</sup>

The azide adduct identified in that study is **10**, and  $k_{\text{az}}/k_s$  for **9** at 80 °C is  $310 \text{ M}^{-1}$ .<sup>10</sup> The structure of **10** demonstrates that the charge in **9** is highly delocalized, and  $k_{\text{az}}/k_s$  comparisons to other oxenium ions show that the azide/solvent selectivity of **9** is similar to that of the 4-bipheny-

(11) Richard, J. P.; Jencks, W. P. *J. Am. Chem. Soc.* **1982**, *104*, 4689–4691. Richard, J. P.; Jencks, W. P. *J. Am. Chem. Soc.* **1982**, *104*, 4691–4692. Richard, J. P.; Jencks, W. P. *J. Am. Chem. Soc.* **1984**, *106*, 1383–1396.

(12) Novak, M.; Kahley, M. J.; Eiger, E.; Helmick, J. S.; Peters, H. E. *J. Am. Chem. Soc.* **1993**, *115*, 9453–9460. McClelland, R. A.; Davidse, P. A.; Hadzalic, G. *J. Am. Chem. Soc.* **1995**, *117*, 4173–4174.

**Scheme 4.** Chemistry of the Related Oxenium Ion **9**



lyoxenium ion, **11**.<sup>10</sup> Since **4**, **7**, **9**, and **11** react with  $\text{N}_3^-$  at or near the diffusion-controlled limit, the aqueous solution lifetimes of **4** and **7** and also of **9** and **11** are very similar.<sup>10,12,13</sup> These results show that the 4-(benzothiazol-2-yl) group behaves as a significantly delocalizing and stabilizing substituent for both oxenium and nitrenium ions.

It is now apparent that putative metabolites of antitumor benzothiazoles will give rise to selective, long-lived nitrenium ions in aqueous solution. Although metabolites of carcino-

genic aromatic amines have long been known to generate highly selective nitrenium ion intermediates in aqueous solution,<sup>12</sup> this is, to the best of our knowledge, the first demonstration that a putative metabolite of an antitumor drug also generates such an intermediate. We are continuing this study with an emphasis on the reaction of **4** and related nitrenium ions with biological nucleophiles.

**Acknowledgment.** We thank the Donors of the American Chemical Society Petroleum Research Fund (Grant No. 43176-AC4) and the NIH/NIGMS (Grant No. R15 GM088751-01) for support of this work. K.J.J. thanks Miami University for an HHMI Summer Undergraduate Research Fellowship, and S.C.B. thanks the OCUR-REEL program supported by the Chemical Division of NSF for an undergraduate summer research fellowship. The support of the NSF in Columbus and the OSU Center for Chemical and Biophysical Dynamics is greatly appreciated.

**Supporting Information Available:** Experimental details, a table of rate constants, Figure S1 showing the decay of the absorbance in  $\text{O}_2$ -saturated phosphate buffer, synthesis of **2** and **3**, and NMR spectra of **2** and **3**. This material is available free of charge via the Internet at <http://pubs.acs.org>.

OL901959Z

(13) Novak, M.; Glover, S. A. *J. Am. Chem. Soc.* **2004**, *126*, 7748–7749. Wang, Y.-T.; Wang, J.; Platz, M. S.; Novak, M. *J. Am. Chem. Soc.* **2007**, *129*, 14566–14567.